IMPLEMENTING THE STANDARD SPECTRUM METHOD FOR ANALYSIS OF β–γ COINCIDENCE SPECTRA

Steven R. F. Biegalski[1], Adam E. Flory[2], Brian T. Schrom[2], James H. Ely[2], Derek A. Haas[2], Theodore W. Bowyer[2], and James C. Hayes[2]

University of Texas at Austin[1] and Pacific Northwest National Laboratory[2]

Sponsored by the National Nuclear Security Administration

Award No. DE-AC05-RL01830/PL10-ASAR-NDD05

ABSTRACT

The standard spectral deconvolution analysis tool (SDAT) algorithms were developed and tested at the University of Texas at Austin. These algorithms utilize the standard spectrum technique for spectral analysis of β–γ coincidence spectra for nuclear explosion monitoring. Work has been conducted under this project to implement these algorithms into a useable scientific software package with a graphical user interface. Improvements include the ability to read in pulse height data (PHD) format, gain matching, and data visualization. New auto-calibration algorithms were developed and implemented based on ^{137}Cs spectra for assessment of the energy vs. channel calibrations. Details on the user tool and testing are included.

OBJECTIVES

In this work algorithms developed to utilize the standard spectrum method for β-γ coincidence spectral analysis were implemented into a user friendly graphical user interface (GUI). Spectra are read in the International Monitoring System (IMS) PHD format. The final result is activity concentration (mBq m^{-3}) for ^{131m}Xe, ^{133m}Xe, ^{133}Xe, and ^{135}Xe. The activity concentration calculations take into account the parent-daughter relationship for ^{133m}Xe and ^{133}Xe, respectively. A spectral gain shifting algorithm and an automatic energy calibration algorithm (based on ^{137}Cs) are also implemented.

RESEARCH ACCOMPLISHED

Background

The Comprehensive Nuclear-Test-Ban Treaty (CTBT) currently defines two detector options for radioxenon detection within the International Monitoring System (IMS) network (Bowyer et al., 2002). The first detector option is the β-γ coincidence spectroscopy system. The advantage of β-γ coincidence spectroscopy is the reduction in background. In addition, such systems facilitate the acquisition of an extra dimension within the spectrum that enables the discrimination of different conversion electron energies that are in coincidence with the *c.a.* 30 keV X-rays. The second detector type is a high resolution gamma-ray spectroscopy system such as a high purity germanium (HPGe) detector. For the IMS network, the radioxenon systems including detector must have a detection limit of 1 mBq $m^{-3}$for ^{133}Xe. All systems must be capable of monitoring ^{131m}Xe, ^{133m}Xe, ^{133}Xe, and ^{135}Xe.

One of the first of β-γ coincidence spectroscopy systems, the Automated Radioxenon Sampler/Analyzer (ARSA) (Bowyer et al., 1999), was produced at Pacific Northwest National Laboratory. The ARSA detector has dual NaI(Tl) detectors surrounding four cells with BC 404 scintillating plastic, as shown in Figure 1. Radioxenon is injected into the cell after being purified from air. The BC 404 scintillating plastic measures the β particles and conversion electrons. The two NaI(Tl) detectors measure gamma-rays and X-rays. Electronics monitor the signals for coincidence events between the BC 404 scintillating plastic and the NaI(Tl) detectors. Such coincidence events are stored in a 256 x 256 channel histogram.

Figure 2 shows a β-γ coincidence spectrum with all four radioxenons of interest present. Note how the ^{131m}Xe and ^{133m}Xe conversion electron response peaks sit on top of the ^{133}Xe and ^{135}Xe β spectra. It is this interference between signals that makes the analysis of β-γ coincidence spectra so difficult.

The classical way to analyze a radioxenon β-γ coincidence spectrum is through a region-of-interest (ROI) approach. The ROI approach simply sums the net counts within pre-defined regions of the spectrum. In order to account for spectral interferences, count ratios between different regions of the spectrum are utilized. Table 1 summarizes the main interferences that need to be accounted for. ^{135}Xe has the least number of interferences that need to be accounted for during ROI analysis. However, ^{131m}Xe and ^{133m}Xe have interferences from sample components. Each interference correction results in the addition of uncertainty. These uncertainties then sum to increase detection limits.

An alternative to the ROI method is the standard spectrum method. This method utilizes the fact that the sample spectrum is simply the sum of each component:

$$Sample = \sum_{i=1}^{m} (Spectrum\ Component)_i (Magnitude)_i \qquad (1)$$

The radioxenon the β-γ coincidence spectra are composed of six main components:

1) Detector Background
2) Radon
3) ^{131m}Xe
4) ^{133m}Xe
5) ^{133}Xe
6) ^{135}Xe

With this limited set of possible inputs, an over-determined system exists and the magnitude for each component may be numerically determined. This work utilizes a least-squares method for solution of the magnitude of each component. The advantage of this method is that all the spectral interferences are directly accounted for. As a result, the standard spectrum method is superior to the ROI method for determining the ^{131m}Xe and ^{133m}Xe counts within a spectrum (Biegalski et al., 2009). Since ^{131m}Xe and ^{133m}Xe have significant value for source discrimination of anthropogenic nuclear sources (Biegalski *et al.*, 2010), efforts are necessary for quantification of these isotopes with the least amount of uncertainty.

Code Features

The standard Spectral Deconvolution Algorithm Tool (SDAT) analysis first step is to utilize a least-squares algorithm to solve for the magnitude of each library vector within both a sample spectrum and a background spectrum. The vector magnitudes are then converted to spectrum counts by multiplying the magnitude by the total counts in the library vector. Due to the detector memory effect, the sample spectrum counts must be adjusted to account for radioxenon activity present in the detector from past samples.

For radionuclides that do not have a parent (^{131m}Xe, ^{133m}Xe, and ^{135}Xe), Equation 2 is used to calculate the counts that must be subtracted:

$$SBKCounts_1 = \frac{BKCounts_1}{\left(1-e^{-\lambda_1 t_{bka}}\right)}\left(e^{-\lambda_1 t_{md}}\right)\left(1-e^{-\lambda_1 t_a}\right) \qquad (2)$$

where,

λ - decay constant (s^{-1})

ε - detector β–γ efficiency for respective radionuclide

BR - β–γ branching ratio for decay of respective radionuclide

t_{bka} - time of background spectrum acquisition (s)

t_{md} - the time difference between the start of the detector memory spectrum acquisition and the start of the sample spectrum acquisition (s)

t_a - the time of the sample spectrum acquisition (s)

BKCounts – counts for each respective nuclide in background spectrum.

For radionculides that have a radioxenon parent (e.g., ^{133}Xe), Equation 3 is used to calculate the counts which must be subtracted. In this notation, the subscript 1 represents the parent radionuclide and subscript 2 represents the daughter radionuclide.

$$SBKCounts_2 = \epsilon_2 BR_2 \left[\frac{BKCounts_1}{\epsilon_1 BR_1 (1-e^{-\lambda_1 t_{bka}})} \left[\frac{\lambda_2}{\lambda_2-\lambda_1} \left(e^{-\lambda_1 t_{md}}\right)\left(1-e^{-\lambda_1 t_a}\right) - \frac{\lambda_1}{\lambda_2-\lambda_1}\left(e^{-\lambda_2 t_{md}}\right)\left(1-e^{-\lambda_2 t_a}\right)\right] + \frac{BKCounts_2 \left(e^{-\lambda_2 t_{md}}\right)\left(1-e^{-\lambda_2 t_a}\right)}{\epsilon_2 BR_2 \left(1-e^{-\lambda_2 t_{bka}}\right)} - \left(\frac{\lambda_2}{\lambda_2-\lambda_1}\right) \frac{BKCounts_1 \left(e^{-\lambda_2 t_{md}}\right)\left(1-e^{-\lambda_2 t_a}\right)}{\epsilon_1 BR_1 \left(1-e^{-\lambda_2 t_{bka}}\right)} - \left(\frac{\lambda_1}{\lambda_2-\lambda_1}\right) \frac{BKCounts_1 \left(e^{-\lambda_2 t_{md}}\right)\left(1-e^{-\lambda_2 t_a}\right)}{\epsilon_1 BR_1 \left(1-e^{-\lambda_1 t_{bka}}\right)} \right] \quad (3)$$

After the detector background (memory effect) is subtracted, the activity concentration is calculated. For radionuclides that do not have a parent (^{131m}Xe, ^{133m}Xe, and ^{135}Xe), Equation 4 is utilized:

$$AC_1 = \frac{Counts_1 {\lambda_1}^2}{\epsilon_1 BR_1 F \left(1-e^{-\lambda_1 t_c}\right)\left(e^{-\lambda_1 t_d}\right)\left(1-e^{-\lambda_1 t_a}\right)} \quad (4)$$

where:

AC - Atmospheric concentration (Bq m^{-3})

F - flow rate of sampler (m^3 s^{-1}). Sampled gas volume may be calculated as the volume of Xe gas (m^3) measured in the sample (normalized to STP) divided by the volumetric concentration of Xe in the atmosphere (87 x 10^{-9} parts Xe per part air) The sampled gas volume (m^3) is then divided by the sample collection time, t_c, (s) to achieve flow rate (m^3 s^{-1}).

λ - decay constant (s^{-1})

ε - detector β–γ efficiency for respective radionuclide

BR - β–γ branching ratio for decay of respective radionuclide

t_c - time of sample collection (s)

t_d - time of sample decay or processing time (s)

t_a - time of spectrum acquisition (s)

Counts - memory corrected counts in sample spectrum

For radionuclides with a radioxenon parent (^{133}Xe) Equation 5 is utilized.

$$AC_2 = \frac{(\lambda_2)^2}{F\left(1-e^{-\lambda_2 t_c}\right)\left(e^{-\lambda_2 t_d}\right)\left(1-e^{-\lambda_2 t_a}\right)} \left[\frac{Counts_2}{\epsilon_2 BR_2} - \frac{Counts_1 \lambda_1 \lambda_2 \left(1-e^{-\lambda_1 t_c}\right)}{\epsilon_1 BR_1 (\lambda_2-\lambda_1)\left(1-e^{-\lambda_1 t_c}\right)\left(e^{-\lambda_1 t_d}\right)\left(1-e^{-\lambda_1 t_a}\right)} \left[\frac{e^{-\lambda_1 t_d}}{\lambda_1}\left(1-e^{-\lambda_1 t_a}\right) - \frac{e^{-\lambda_2 t_d}}{\lambda_2}\left(1-e^{-\lambda_2 t_a}\right)\right] - \frac{Counts_1 \lambda_1 \left[(\lambda_1-\lambda_2)+\lambda_2 e^{-\lambda_1 t_c} - \lambda_1 e^{-\lambda_2 t_c}\right]\left(e^{-\lambda_2 t_d}\right)\left(1-e^{-\lambda_2 t_a}\right)}{\epsilon_1 BR_1 \lambda_2 (\lambda_1-\lambda_2)\left(1-e^{-\lambda_1 t_c}\right)\left(e^{-\lambda_1 t_d}\right)\left(1-e^{-\lambda_1 t_a}\right)} \right] \quad (5)$$

The next step is to calculate uncertainty in the activity concentration. Again, this requires different equations for radionuclides with and without radioactive parents. The activity concentration uncertainty for radionuclides without parents is shown in Equation 6:

$$\sigma_{AC_1} = AC_1 \left(\frac{{\lambda_1}^2}{\left(1-e^{-\lambda_1 t_c}\right)\left(e^{-\lambda_1 t_d}\right)\left(1-e^{-\lambda_1 t_a}\right)} \right) \sqrt{\left[\left(\frac{\sigma_{Counts_1}}{Counts_1}\right)^2 + \left(\frac{\sigma_{\epsilon_1}}{\epsilon_1}\right)^2 + \left(\frac{\sigma_{BR_1}}{BR_1}\right)^2 + \left(\frac{\sigma_F}{F}\right)^2 \right]} \quad (6)$$

The uncertainty in activity concentration for radionuclides with a parent (e.g., ^{133}Xe) is provided in Equation 7:

$$\sigma_{AC_2} = \sqrt{\begin{array}{c}(Z_1)^2\left(\frac{Counts_2}{\epsilon_2 BR_2 F}\right)^2\left[\left(\frac{\sigma_{Counts_2}}{Counts_2}\right)^2+\left(\frac{\sigma_{\epsilon_2}}{\epsilon_2}\right)^2+\left(\frac{\sigma_{BR_2}}{BR_2}\right)^2+\left(\frac{\sigma_F}{F}\right)^2\right]\\ +(Z_1Z_3+Z_1Z_2)^2\left(\frac{Counts_1}{\epsilon_1 BR_1 F}\right)^2\left[\left(\frac{\sigma_{Counts_1}}{Counts_1}\right)^2+\left(\frac{\sigma_{\epsilon_1}}{\epsilon_1}\right)^2+\left(\frac{\sigma_{BR_1}}{BR_1}\right)^2+\left(\frac{\sigma_F}{F}\right)^2\right]\end{array}} \quad (7)$$

where,

$$Z_1 = \frac{(\lambda_2)^2}{(1-e^{-\lambda_2 t_c})(e^{-\lambda_2 t_d})(1-e^{-\lambda_2 t_a})}$$

$$Z_2 = \frac{\lambda_2\lambda_1\left(1-e^{-\lambda_1 t_c}\right)}{(\lambda_2-\lambda_1)(1-e^{-\lambda_1 t_c})(e^{-\lambda_1 t_d})(1-e^{-\lambda_1 t_a})}\left[\frac{e^{-\lambda_1 t_d}}{\lambda_1}\left(1-e^{-\lambda_1 t_a}\right)-\frac{e^{-\lambda_2 t_d}}{\lambda_2}\left(1-e^{-\lambda_2 t_a}\right)\right]$$

$$Z_3 = \frac{\lambda_1\left[(\lambda_1-\lambda_2)+\lambda_2 e^{-\lambda_1 t_c}-\lambda_1 e^{-\lambda_2 t_c}\right]\left(e^{-\lambda_2 t_d}\right)\left(1-e^{-\lambda_2 t_a}\right)}{\lambda_2(\lambda_1-\lambda_2)(1-e^{-\lambda_1 t_c})(e^{-\lambda_1 t_d})(1-e^{-\lambda_1 t_a})}$$

Lastly the critical limit, detection limit, and minimum detectable concentrations are calculated. The calculation method is based off of the Currie method (Currie, 1969). Equations 8, 9, 10, and 11 show the equations to calculate the critical limit (L_c), detection limit (L_D), and minimum detectable concentrations (MDC), respectively. Note that the critical limit and detection limit equations are independent of parent/daughter relationships within the radioxenon isotopes. The minimal detectable concentration calculation does change if a radioactive parent is present.

$$\mathrm{L_C} = \mathrm{k}\sqrt{\mu_\mathrm{I} + \mu_\mathrm{M} + (\sigma_\mathrm{I})^2 + (\sigma_\mathrm{M})^2} \quad (8)$$

where,

μ_I - interference signal

μ_M - memory effect signal

σ_I - interference signal standard deviation

σ_M - memory effect signal standard deviation

$$\mathrm{L_D} = \mathrm{k}^2 + 2\mathrm{L_C}. \quad (9)$$

where,

k - abscissas of the Normal distrbution (usually at 95% confidence)

$$MDC_1 = \frac{L_{D_1}{\lambda_1}^2}{\epsilon_1 BR_1 F\left(1-e^{-\lambda_1 t_c}\right)\left(e^{-\lambda_1 t_d}\right)\left(1-e^{-\lambda_1 t_a}\right)} \quad (10)$$

$$MDC_2 = \frac{(\lambda_2)^2}{F\left(1-e^{-\lambda_2 t_c}\right)\left(e^{-\lambda_2 t_d}\right)\left(1-e^{-\lambda_2 t_a}\right)}\left[\frac{L_{D_2}}{\epsilon_2 BR_2}-\frac{Counts_1\lambda_1\lambda_2\left(1-e^{-\lambda_1 t_c}\right)}{\epsilon_1 BR_1(\lambda_2-\lambda_1)\left(1-e^{-\lambda_1 t_c}\right)\left(e^{-\lambda_1 t_d}\right)\left(1-e^{-\lambda_1 t_a}\right)}\left[\frac{e^{-\lambda_1 t_d}}{\lambda_1}\left(1-e^{-\lambda_1 t_a}\right)-\frac{e^{-\lambda_2 t_d}}{\lambda_2}\left(1-e^{-\lambda_2 t_a}\right)\right]-\frac{Counts_1\lambda_1\left[(\lambda_1-\lambda_2)+\lambda_2 e^{-\lambda_1 t_c}-\lambda_1 e^{-\lambda_2 t_c}\right]\left(e^{-\lambda_2 t_d}\right)\left(1-e^{-\lambda_2 t_a}\right)}{\epsilon_1 BR_1\lambda_2(\lambda_1-\lambda_2)\left(1-e^{-\lambda_1 t_c}\right)\left(e^{-\lambda_1 t_d}\right)\left(1-e^{-\lambda_1 t_a}\right)}\right] \quad (11)$$

SDAT GUI

The SDAT GUI was written in C#. Figure 3 provides a screen shot of the SDAT GUI showing a sample spectrum with ^{131m}Xe and ^{133}Xe. The β-γ coincidence spectrum, summed β spectrum, and summed γ spectrum are all visualized. The sample is not analyzed due to lack of detector calibration data at this point. If the sample was analyzed, the activity concentrations, their associated uncertainty, and MDCs would be provided at the bottom of the GUI.

Figure 4 shows a screenshot of the re-calibration screen within the SDAT GUI. Re-calibration is necessary to adjust the energy vs. channel calibration on both the β and γ axes. The gain of the sample spectrum must match that of the library calibration files. If these calibrations do not match, then SDAT will not correctly fit the sample spectrum. The re-calibration works by entering the current energy vs. channel calibration (fit to a linear equation) of the sample spectrum. This sample calibration may be calculated from the header information within the sample spectrum or may be obtained from an "Auto-Cal" subroutine that evaluates the most recent ^{137}Cs quality control spectrum. A target energy vs. channel calibration is provided in the header information of the calibration library PHD files. Once the sample is gain shifted, then analysis of the spectra may be performed.

CONCLUSIONS AND RECOMMENDATIONS

The original SDAT algorithms were tested in-depth. However, after implementation into a GUI detector calibrations need to be evaluated for detector systems of interest. Testing will include a controlled laboratory data set as well as a large set of field data from the IMS. The sensitivity of detector calibration is also being investigated. Once completed, SDAT should provide a robust tool for scientific evaluation and analysis of radioxenon β-γ coincidence spectra.

REFERENCES

Biegalski, S.R.F, K.M. Foltz Biegalski, D. Haas (2009) SDAT: Analysis of ^{131m}Xe with ^{133}Xe interference, *J. Radioanal. Nucl. Chem.* 282:3, 715–719.

Biegalski, S.R., T. Saller, J. Helefand, K.M.F. Biegalski (2010) Sensitivity study on modeling radioxenon signals from radiopharmaceutical production facilities, *J. Radioanal. Nucl. Chem.* 284:3, 663–668.

Bowyer T.W., K.H. Abel, C.W. Hubbard, A.D. McKinnon, M.E. Panisko, R.W. Perkins, P.L. Reeder, R.C. Thompson, R.A. Warner (1999), Automated Separation and Measurement of Radioxenon for Monitoring a Comprehensive Test Ban Treaty, *J. Radioanal. Nucl. Chem.* 240:1, 109–122.

Bowyer T.W., C. Schlosser, K.H. Abel, M. Auer, J.C. Hayes, T.R. Heimbinger, J.I. McIntyre, M.E. Panisko, P.L. Reeder, H. Satorius, J. Schulze, W.Weiss (2002), Detection and analysis of xenon isotopes for the comprehensive nuclear-test-ban treaty international monitoring system, *J. Envir. Radio.*, 59: 2: 139–151.

Reeder P.L., T.W. Bowyer, J.I McIntyre, W.K. Pitts, A. Ringbom, C. Johansson (2004) "Gain calibration of a β/γ coincidence spectrometer for automated radioxenon analysis, *Nucl. Inst. Meth Phys. Res.:A*, 521:2-3, 586–599.

Table 1. Radioxenon β-γ spectral interferences.

	Regions for Quantification of Radionuclide by ROI Method		**Interferences that must be accounted for**					
	Gamma Detector	**Beta Cell**	**Detector Background**	**Radon**	**^{131m}Xe**	**^{133m}Xe**	**^{133}Xe**	**^{135}Xe**
^{131m}Xe	30 keV	164 keV	X	X		X	X	X
^{133m}Xe	30 kev	233 keV	X	X	X		X	X
^{133}Xe	81 keV	0 – 346 keV	X	X				X
^{135}Xe	250 keV	0 – 910 keV	X	X				

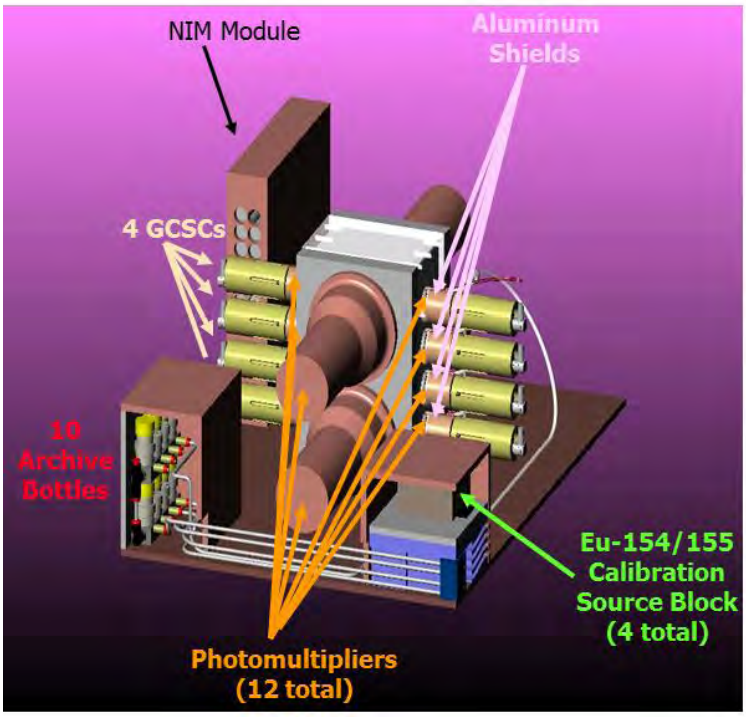

Figure 1. Schematic of the NaI(Tl)-plastic based β-γ coincidence spectrometer used in the ARSA system.

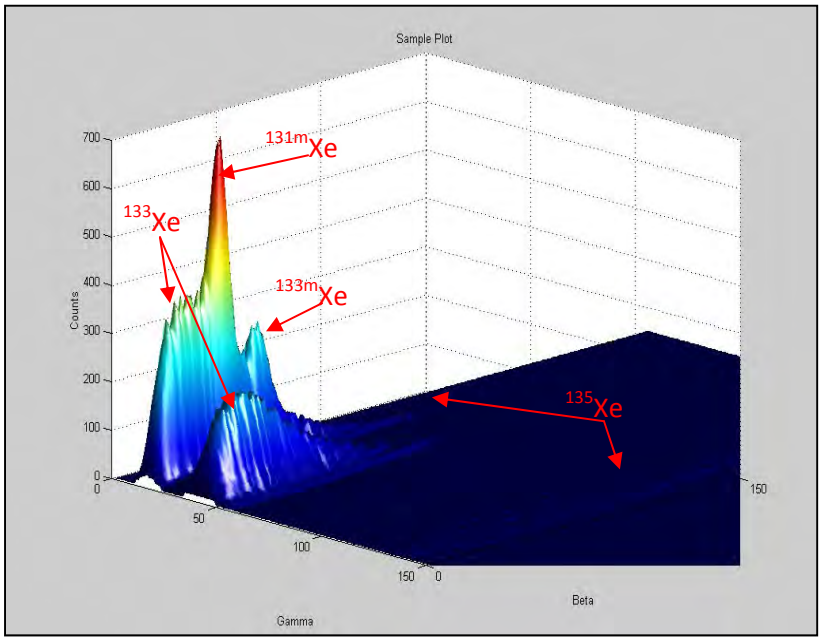

Figure 2. Actual β-γ spectrum from the ARSA system showing four of the four xenon isotopes of interest.

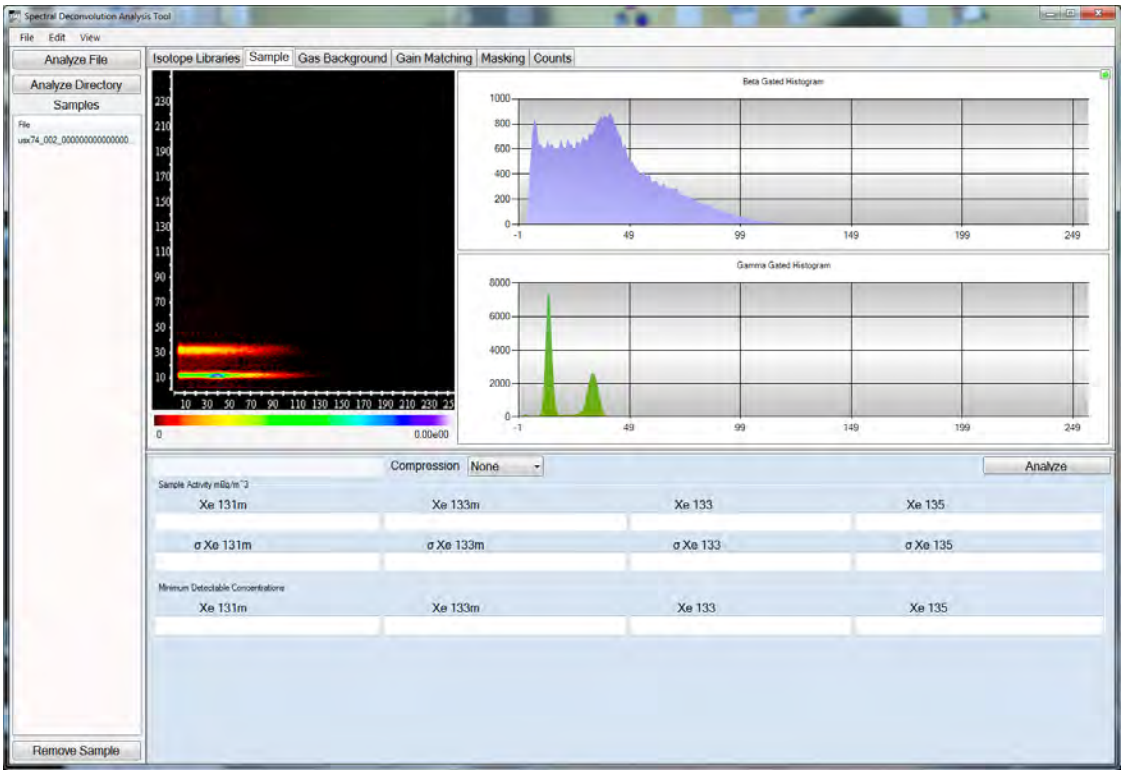

Figure 3. Sample spectrum view in SDAT of sample with ^{131m}Xe and ^{133}Xe.

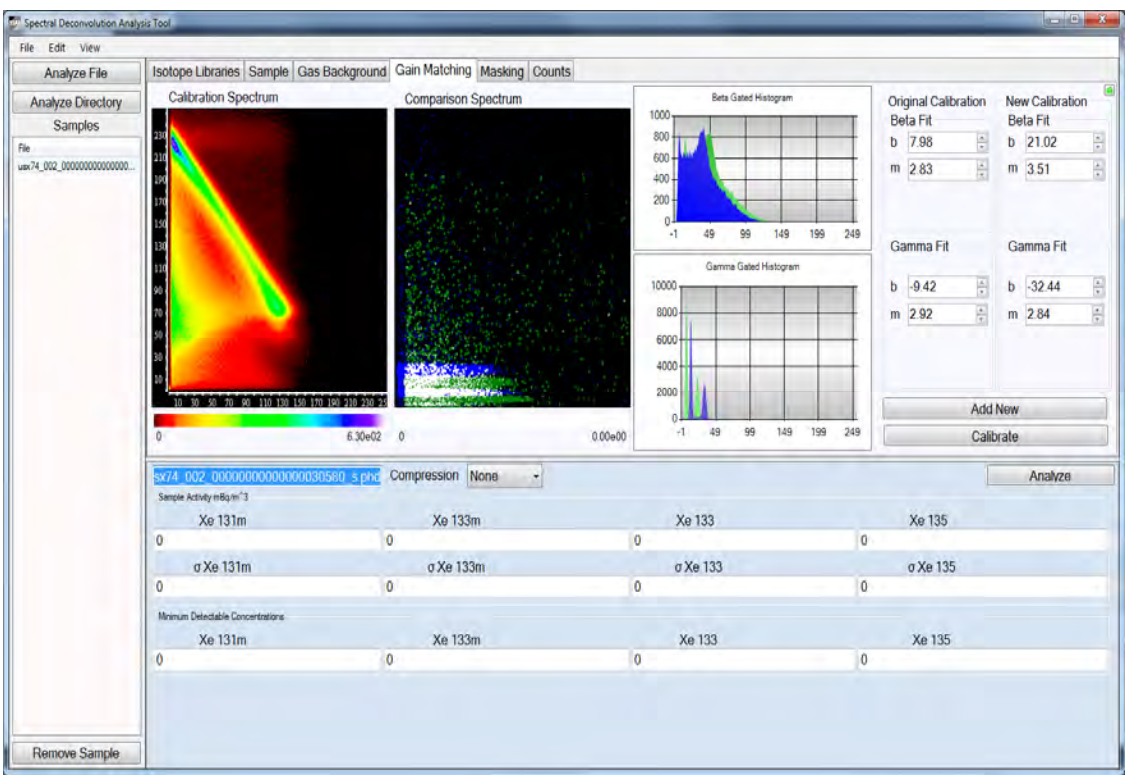

Figure 4. Re-calibration screen from SDAT GUI.